Kinetic description of microwave Raman regime free-electron laser in the presence of helical wiggler and guiding magnetic fields

P.K. MISHRA

Central Mining Research Institute, Barwa Road, Dhanbad-826001, India;
e-mail: mishrapkapp@yahoo.co.in

A full dispersion relation obtained for free-electron laser by kinetic approach based on the method of characteristics in the presence of circularly polarized, periodic, static helical wiggler magnetic field and guide magnetic field incorporating the detailed relativistic particle trajectories is reduced to Raman regime approximations. The temporal and spatial growth rates are evaluated in microwave region. A detailed analysis has been done for temporal and spatial growth rates in Raman regime, especially for microwave region. The spatial growth rate is more than that of temporal growth. The results have been compared with available results obtained by other techniques.

Keywords: free electron laser, kinetic approach, microwave, wiggler, guide magnetic field, Raman regime, temporal, spatial.

1. Introduction

The wave amplification in free-electron lasers has been thoroughly studied in a configuration consisting of helical wiggler and guide magnetic fields [1]. The use of the axial guide field was originally considered for enhancing the focusing of intense electron beam. It also enhances transverse wiggler velocity and increases both the gain and efficiency of the interaction. The Raman regime is characterized by collective interaction between the electrons for high electron beam current and low electron energy. In free-electron lasers, the electron oscillates in the buckets of the pondermotive potential with the synchrotron frequency. These oscillations get mixed with the emission and absorption processes to create radiation at frequencies shifted from fundamentals by the synchrotron frequency. At sufficiently high intensity, gain is observed on the long wavelength sideband. Because of this analogy to the molecular Raman effect, the free-electron laser synchrotron instability is sometimes referred to as Raman instability.

BERNSTEIN and FRIEDLAND [2], KWAN and DAWSON [3], UHM and DAVIDSON [4], YIN and BEKEFI [5] and QIAN *et al.* [6] have studied free-electron lasers in Raman regime

using hydrodynamic approach in the presence of planar wiggler and helical wiggler fields. Davies *et al.* studied Compton and Raman free-electron laser instability for a cold [7] and warm [8] electron beam propagating through helical wiggler without a guide magnetic field using kinetic and vector potential approaches. Roberson and Sprangle [9] carried out a review on free-electron lasers in Compton and Raman regimes using hydrodynamic approach with and without the guide magnetic field. The kinetic description of low gain free-electron laser has also been investigated using Einstein coefficient method incorporation with detailed particle trajectories for perfect and imperfect injections of a beam in a circularly polarized, static, periodic helical wiggler and axial guide magnetic fields [10].

Therefore, in the present paper, free-electron laser instability is studied by kinetic approach incorporating the details of particle trajectories, using the method of characteristics, in the helical wiggler and guide magnetic fields. The dispersion relation obtained [11] is reduced to Raman regime dispersion relation [12] for the upper shifted frequencies. Temporal and spatial growth rates are obtained from Raman regime dispersion relation in microwave region for the same plasma frequency and cavity parameters. Further temporal and spatial growth rates are studied in detail.

2. Full dispersion relation

All the components of dielectric tensor have been obtained [11] for tenuous electron beam with finite spread in horizontal and vertical velocities. With the help of these tensors, while neglecting smaller order terms and after some algebraic manipulations, the full dispersion relation (FDR) is obtained as:

$$\left\{ \omega^2 - k_z^2 c^2 - \frac{\omega_p^2}{\gamma_0} \frac{(\omega - k_z v_{z0})^2}{(\omega - k_z v_{z0})^2 - \Omega^2} \right\} \left\{ \omega^2 - (k_z + 2k_0)^2 c^2 - \frac{\omega_p^2}{\gamma_0} \frac{(\omega - k_z v_{z0})^2}{(\omega - k_z v_{z0})^2 - \Omega^2} \right\}$$

$$\times \left\{ \left[\omega^2 - (k_z + k_0) v_{z0} \right]^2 - \frac{\omega_p^2}{\gamma_0 \gamma_z^2} \right\} =$$

$$= -\frac{\hat{\omega}_c^2 \omega_p^2}{\gamma_0 (1 - \hat{\Omega})^2} \left\{ \omega^2 - (k_z + k_0)^2 c^2 - \frac{\omega_p^2}{\gamma_0} \right\}$$

$$\times \left\{ \omega^2 - (k_z + k_0)^2 c^2 - k_0^2 c^2 - \frac{\omega_p^2}{\gamma_0} \frac{(\omega - k_z v_{z0})^2}{(\omega - k_z v_{z0})^2 - \Omega^2} \right\} \tag{1}$$

where

$$\hat{\omega}_c = \frac{eB_w}{\gamma_0 mc^2 k_0}, \qquad \hat{\Omega} = \frac{\Omega}{k_0 v_{z0}} \quad \text{and} \quad \gamma_z = \left(1 - \frac{v_z^2}{c^2}\right)^{-\frac{1}{2}} \tag{2}$$

Now, when the guide field is put to zero, our expression (1) for FDR reduces exactly to that of DAVIDSON [13].

3. Dispersion relation in Raman regime

When the beam density is sufficiently high, the longitudinal electric field E_z plays an important role in determining detailed properties of free-electron laser instability. In this case, a more accurate analysis of the full dispersion relation shown in Eq. (1) is required, which includes the effects of the longitudinal plasma oscillations occurring in the dielectric factor $\{[\omega - (k_z + k_0)v_{z0}]^2 - \omega_p^2/\gamma_0\gamma_z^2\}$. In the vicinity of the growth rate maximum, one approximates the electrostatic part of the full dispersion relation appearing in the third bracket on the left-hand side as:

$$\left[\omega - (k_z + k_0)v_{z0}\right]^2 - \gamma_0\gamma_z^2 = -\frac{2\omega_p}{\gamma_0^{1/2}\gamma_z}\left[\omega - (k_z + k_0)v_{z0} + \frac{\omega_p}{\gamma_0^{1/2}\gamma_z}\right] \tag{3}$$

The electromagnetic part of the full dispersion relation, appearing in the first bracket on the left-hand side, is obtained making use of approximations $\omega - (k_z + k_0) = v_{z0}$ in the Doppler shifted frequency and subsequently replacing $\omega \approx ck_z$ in the electromagnetic term as:

$$\left\{\omega^2 - k_z^2 c^2 + \frac{\omega_p^2}{\gamma_0}\frac{(\omega - k_z v_{z0})^2}{(\omega - k_z v_{z0})^2 - \Omega^2}\right\} =$$

$$= \omega^2 - \left[k_z^2 c^2 + \frac{\omega_p^2}{\gamma_0(1 - \hat{\Omega})^2}\right] =$$

$$= 2\left\{k_z^2 c^2 + \frac{\omega_p^2}{\gamma_0(1 - \hat{\Omega})^2}\right\}^{\frac{1}{2}}\left\{\omega - \left[k_z^2 c^2 + \frac{\omega_p^2}{\gamma_0(1 - \hat{\Omega})^2}\right]^{\frac{1}{2}}\right\} \tag{4}$$

The remaining factor of ω^2 in brackets on the left-hand side and the right-hand side of Eq. (1) is also approximated considering the resonance condition as:

$$\omega^2 = k_z^2 c^2 + \frac{\omega_p^2}{\gamma_0} \frac{(\omega - k_z v_{z0})^2}{(\omega - k_z v_{z0})^2 - \Omega^2}$$

The approximation mentioned above and algebraic manipulations reduce the full dispersion relation given in Eq. (1) to Raman regime as:

$$\left\{ \omega - (k_z + k_0)v_{z0} + \frac{\omega_p}{\gamma_0^{1/2}\gamma_z} \right\} \left\{ \omega - \left[k_z^2 c^2 + \frac{\omega_p^2}{\gamma_0(1 - \hat{\Omega}^2)} \right]^{\frac{1}{2}} \right\} =$$

$$= -\frac{\hat{\omega}_c^2 \gamma_z}{4\gamma_0^{1/2}} \frac{\omega_p}{(1 - \hat{\Omega})^2} \frac{k_0 c \left(2k_z c + k_0 c + \frac{\hat{\Omega}^2 \omega_p^2}{1 - \hat{\Omega}^2} \right)}{\left[k_z^2 c^2 + \frac{\omega_p^2}{\gamma_0(1 - \hat{\Omega}^2)} \right]^{\frac{1}{2}}} =$$

$$= -R \tag{5}$$

Equation (5) may be reduced to a simple quadratic equation as:

$$\omega^2 - \mu \omega - R = 0 \tag{6}$$

with R, the coupling term, being defined on right-hand side of Eq. (5) and

$$\mu = \left[k_z^2 c^2 + \frac{\omega_p^2}{\gamma_0(1 - \hat{\Omega}^2)} \right]^{\frac{1}{2}} - (k_z + k_0)v_{z0} + \frac{\omega_p}{\gamma_0^{1/2}\gamma_z} \tag{7}$$

where μ may be defined as the frequency mismatch between the electrostatic and electromagnetic waves.

Equation (5) is often referred to as the Raman regime dispersion relation. If one considers electromagnetic waves with frequency less than the Doppler-shifted cyclotron frequency, the dispersion relation is approximately given by $\omega = ck_z$. By setting the coupling coefficient R equal to zero, one obtains the uncoupled electrostatic and electromagnetic waves. At the intersection of the dispersion curves, where the wave number and frequency matching conditions are satisfied, negative energy electrostatic beam mode and positive energy electromagnetic wave are strongly coupled together and, therefore, give rise to instability [11].

By expanding Eq. (6) about $(\overline{\omega}, k)$ at which electrostatic and electromagnetic dispersion relations are simultaneously satisfied, one determines the frequency $\omega = \overline{\omega} + \delta\omega$ for $k = \overline{k}$ of the unstable electromagnetic wave [13]. The procedure yields the solution:

$$\delta\omega = \frac{\mu \pm i(4R - \mu^2)^{1/2}}{2} \tag{8}$$

Thus solution of the dispersion relation (6) reduces to:

$$\omega = (k_z + k_0)v_{z0} - \frac{\omega_p}{\gamma_0^{1/2}\gamma_z} + \frac{\mu}{2} \pm \frac{i(4R - \mu^2)^{1/2}}{2} \tag{9}$$

Equation (9) indicates that the electromagnetic wave is unstable and the width of the unstable spectrum is determined by the various parameters, such as the beam energy and the strength of the wiggler field and the axial guide magnetic field.

3.1. Temporal growth rate of free-electron laser

The dimensionless temporal growth rate is given by [7, 12, 13]:

$$\frac{\mathrm{Im}\,\omega}{ck_0} = \frac{i(4R - \mu^2)^{1/2}}{2ck_0} \tag{10}$$

and

$$\mathrm{Re}\,\omega = (k_z + k_0)v_{z0} - \frac{\omega_p}{\gamma_0^{1/2}\gamma_z} + \frac{\mu}{2} \tag{11}$$

From Equation (5), it is seen that R is proportional to $\hat{\omega}_c^2$; therefore, the width of unstable spectrum is linearly dependent on the strength of the helical wiggler magnetic field. When the axial guide magnetic field is withdrawn from Eq. (10), the expression reduces to that of DAVIDSON [13].

3.2. Spatial growth rate of free-electron laser

The dimensionless spatial growth rate is given as:

$$\frac{k_i}{k_0} = -\frac{\mathrm{Im}\,\omega/ck_0}{1/c\frac{\partial\omega}{\partial k_z}} \tag{12}$$

The expression for absolute instability in Raman regime obtained in Eq. (10) and group velocity is determined from Equation (11) under approximation $\omega \cong ck_z$ and gives the spatial growth rate with $\hat{\omega} = \omega/ck_0$ as:

$$\frac{k_i}{k_0} = \frac{\frac{1}{2}\left\{\frac{\hat{\omega}_c^2 \hat{\omega}_p^2 \gamma_z}{(1-\hat{\Omega})^2} \frac{(1+2\hat{\omega}) + \frac{\hat{\Omega}^2 \hat{\omega}_p^2}{(1-\hat{\Omega})^2}}{\left(\hat{\omega}^2 + \frac{\hat{\omega}_p^2}{1-\hat{\Omega}^2}\right)^{\frac{1}{2}}} - \left[\left(\hat{\omega}^2 + \frac{\hat{\omega}_p^2}{1-\hat{\Omega}^2}\right)^{\frac{1}{2}} - \frac{v_{z0}}{c}(1+\hat{\omega}) + \frac{\hat{\omega}_p^2}{\gamma_z}\right]^2\right\}^{\frac{1}{2}}}{\frac{\frac{\omega}{W} + \frac{v_{z0}}{c}Q}{1-Q}}$$

(13)

where

$$W = \left[\omega^2 + \frac{\omega_p^2}{\gamma_0} \frac{\omega^2\left(1-\frac{v_{z0}}{c}\right)^2}{\omega^2\left(1-\frac{v_{z0}}{c}\right)^2 - \Omega^2}\right]^{\frac{1}{2}}$$

(14)

$$Q = \frac{\omega_p^2}{\gamma_0} \frac{\omega}{W} \frac{\Omega^2\left(1-\frac{v_{z0}}{c}\right)}{\left[\omega^2\left(1-\frac{v_{z0}}{c}\right)^2 - \Omega^2\right]^2}$$

4. Detail analysis of microwave Raman regime

Variation of temporal growth rate in Raman regime with k_z/k_0 for $\gamma_0 = 2$, $\gamma_z = 1.41$, plasma frequency $\hat{\omega}_p = \omega_p/\gamma_0^{1/2}ck_0 = 0.06$, $\omega_c/\gamma_0^{1/2}ck_0 = 0.5$ and $v_{z0}/c = 0.75$ is shown in Fig. 1a for different values of the guide magnetic field $\hat{\Omega}$ being more than one. The real frequency $\hat{\omega} = \omega/ck_0$ plotted on the other axis indicates that the maximum growth rate cuts the real frequency at $k_z/k_0 = 3$ and corresponds to the real frequency $\omega_r = 2.05\times10^{11}$ cm^{-1} and wavelength $\lambda_r = 0.919$ cm. The increase of the guide magnetic field decreases the growth rate as well as widths of the spectrum extending over large k_z/k_0. If the choice is made for $\hat{\Omega} < 1$ then the temporal growth rate increases. The picture is opposite on either side of the resonance value of as $\hat{\Omega}$, shown in Fig. 2a, which indicates variation in the growth rate with guide magnetic field for the same parameter of Fig. 1a. Near the resonance, where $\hat{\Omega} = 1$, which corresponds to the guide magnetic field $B_{\parallel} = 8$ kG, the expression shows singularity

and maximum growth is possible little below the resonance or away from the resonance. The results shown in Figs. 1**a** and 2**a** are in agreement with those obtained by YIN and BEKEFI [5].

Spatial dimensionless growth rate versus ω/ck_0 is shown in Fig. 1**b** for the various dimensionless guide magnetic field parameters $\hat{\Omega} > 1$ in the microwave Raman region. The spatial growth rate is enhanced up to five times compared to the temporal growth rate for the same value of the guide magnetic field having $\hat{\Omega} > 1$. Thus, Fig. 2**a** corresponding to the temporal growth rate and Fig. 2**b** corresponding to the spatial growth rate clearly indicate the choice and role of the guide field for controlling the growth rate.

Figure 3**a** shows variation in the growth rate ($\text{Im}\,\omega/ck_0$) with k_z/k_0 in Raman regime for different values of wiggler magnetic field ω_c for a fixed value of guide magnetic field $\hat{\Omega} = 2$, *i.e.*, $B_\parallel = 16$ kG away from singularity $\hat{\Omega} = 1$. The growth rate
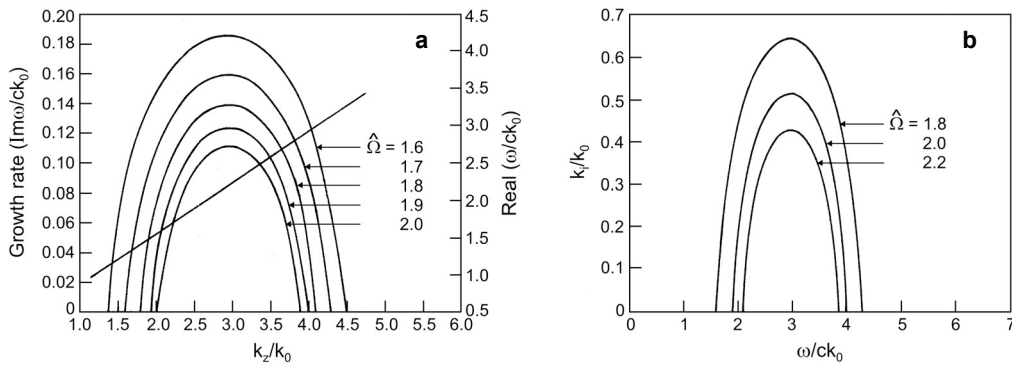

Fig. 1. Dependence of dimensionless: **a** – temporal growth rate on dimensionless wave number for various guide field strengths ($\gamma_0 = 2$, $\hat{\omega}_c = 0.5$, $\hat{\omega}_p = 0.06$), and **b** – spatial growth rate on dimensionless wave number for various guide field strengths ($\gamma_0 = 2$, $\hat{\omega}_c = 0.5$, $\hat{\omega}_p = 0.08$).
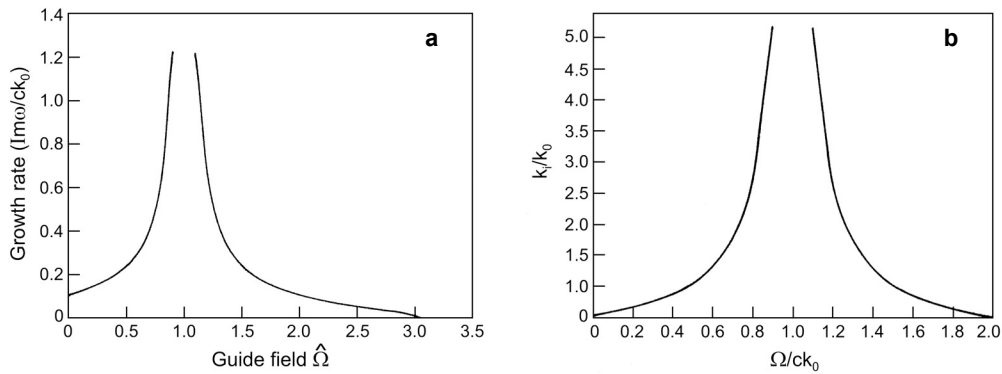

Fig. 2. Dependence of dimensionless: **a** – temporal growth rate on dimensionless guide magnetic field ($\gamma_0 = 2$, $\hat{\omega}_c = 0.5$, $\hat{\omega}_p = 0.08$, $k_z/k_0 = 3$), and **b** – spatial growth rate on dimensionless guide field strength ($\gamma_0 = 2$, $\hat{\omega}_c = 0.5$, $\hat{\omega}_p = 0.08$, $k_z/k_0 = 3$).
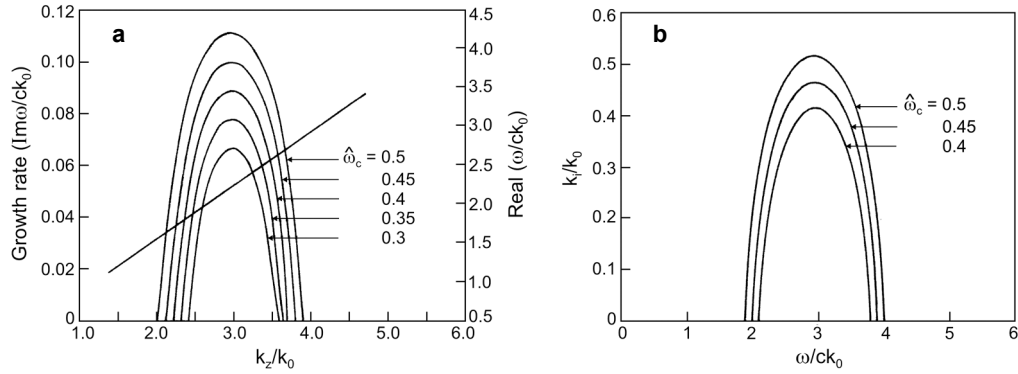
Fig. 3. Dependence of dimensionless: **a** – temporal growth rate on dimensionless wave number for various wiggler magnetic field strengths ($\gamma_0 = 2$, $\hat{\omega}_p = 0.08$, $\hat{\Omega} = 2$), and **b** – spatial growth rate on dimensionless frequency for various wiggler magnetic field strengths ($\gamma_0 = 2$, $\hat{\omega}_p = 0.08$, $\hat{\Omega} = 2$).

increases with an increase of wiggler field, but maxima remain fixed at $k_z/k_0 = 3$, and corresponds to the frequency generated $\omega_r = 2.05\times10^{11}$ cm^{-1} and wavelength of radiation field $\lambda_r = 0.919$ cm, which is the same as in Fig. 1**a**. However, there exists an extremum value of the wiggler field for these parameters to obtain lasing action with sufficient gain. The results are in conformity with those obtained by DEMOKAN and KABAK [14] using the hydrodynamic approach. The results are very sensitive to the parameter chosen for wiggler field, wiggler wave number, beam density and beam energy. One has to search for optimum values of these parameters in the region to obtain a reasonable values of the growth rate.

In Figure 3**b**, spatial growth rate k_i/k_0 versus ω/ck_0 in Raman regime for different values of dimensionless wiggler magnetic fields has been discussed for the same parameters as in the figures mentioned above and a fixed value of the dimensionless guide magnetic field $\hat{\Omega} = 2$. The wiggler magnetic field enhances the growth rate as well as the unstable spectrum of ω/ck_0. The maxima remain at the fixed point for $\omega/ck_0 = 3$.

Figure 4**a** shows the variation in the growth rate (Imω/ck_0) with k_z/k_0 for the different values of dimensionless plasma frequencies $\hat{\omega}_p$ (beam density) and other fixed parameters given in the caption. The increase of the beam density makes the growth rate as well as the width of unstable spectrum increases. The control of beam density is depicted in Fig. 5**a** for temporal growth rate. The growth rate increases and reaches a maximum and then falls, indicating that choice has to be made for a particular value of beam density and energy for generating growth rate and desired wavelength by free-electron laser action. One has to compensate the wiggler magnetic field, guide magnetic field and various other parameters. The results are in agreement with those of KWAN and DAWSON [3].
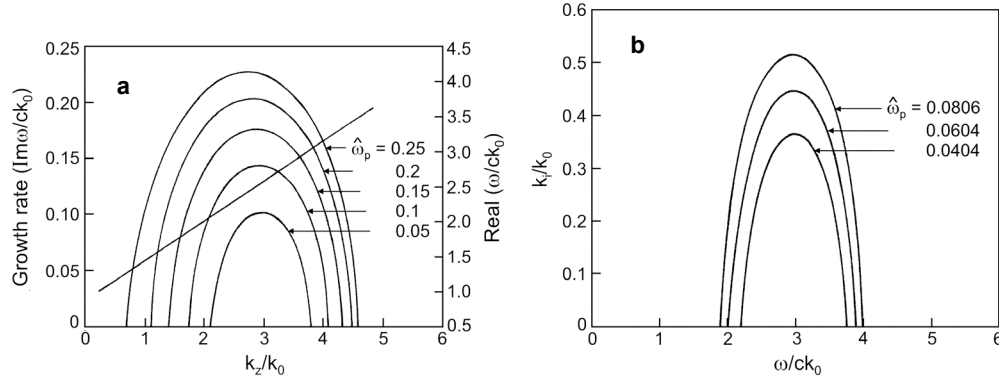
Fig. 4. Dependence of dimensionless: **a** – temporal growth rate on dimensionless wave number for various beam densities ($\gamma_0 = 2$, $\hat{\omega}_c = 0.5$, $\hat{\Omega} = 2$), and **b** – spatial growth rate on dimensionless frequency for various beam densities ($\gamma_0 = 2$, $\hat{\omega}_c = 0.5$, $\hat{\Omega} = 2$).
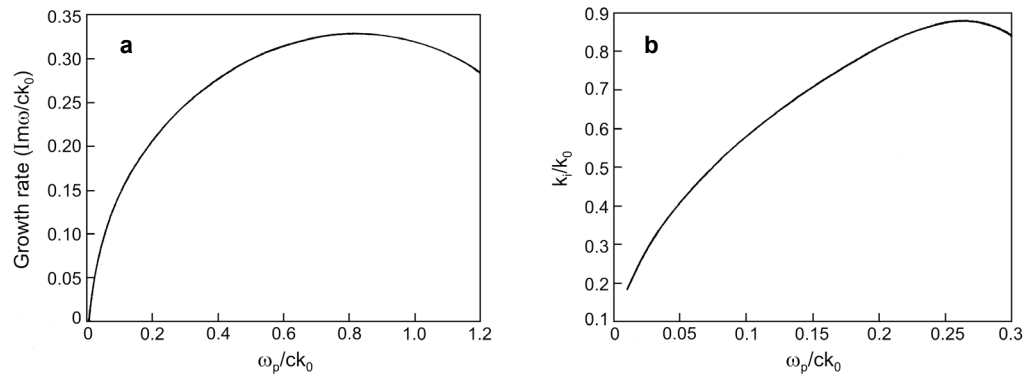

Fig. 5. Dependence of dimensionless: **a** – temporal growth rate on dimensionless plasma frequency ($\gamma_0 = 2$, $\hat{\omega}_c = 0.5$, $\hat{\Omega} = 2$, $k_z/k_0 = 3$), and **b** – spatial growth rate on dimensionless plasma frequency ($\gamma_0 = 2$, $\hat{\omega}_c = 0.5$, $\hat{\Omega} = 2$, $k_z/k_0 = 3$).

The effect of the beam density on dimensionless spatial growth rate k_i/k_0 versus ω/ck_0 for the same parameters and fixed value of dimensionless wiggler field $\omega_c/\gamma_0^{1/2}ck_0 = 0.5$ for different values of dimensionless plasma frequency $\hat{\omega}_p$ (beam density) is shown in Fig. 4**b**. The spatial growth rate and unstable spectrum increase with the increase of beam density. The maxima for spatial growth rate appear at the same point of the axis ω/ck_0. The choice of beam density is very sensitive parameter for obtaining the spatial growth rate as shown in Fig. 5**b**. The growth rate increases with an increase of the dimensionless plasma frequency $\hat{\omega}_p$ up to some extent and then decreases substantially with an increase of $\hat{\omega}_p$. This figure also indicates that

free-electron laser in Raman regime can be tuned for different wavelengths and frequencies of radiations in the microwave region by changing the beam density.

References

[1] FREUND H.P., DAVIDSON R.C., JOHNSTON G.L., *Linear theory of the collective Raman interaction in a free-electron laser with a planar wiggler and an axial guide field*, Physics of Fluids B: Plasma Physics **2**(2), 1990, pp. 427–35.

[2] BERNSTEIN I.B., FRIEDLAND L., *Theory of the free-electron laser in combined helical pump and axial guide fields*, Physical Review A **23**(2), 1981, pp. 816–23.

[3] KWAN T., DAWSON J.M., *Investigation of the free-electron laser with a guide magnetic field*, Physics of Fluids **22**(6), 1979, pp. 1089–103.

[4] UHM H.S., DAVIDSON R.C., *Theory of free-electron laser instability in a relativistic annular electron beam*, Physics of Fluids **24**(8), 1981, pp. 1541–52.

[5] YIN Y.Z., BEKEFI G., *Dispersion characteristic of a free-electron laser with a linearly polarized Wiggler and axial guide field*, Journal of Applied Physics **55**(1), 1984, pp. 33–42.

[6] QUIAN B.-L., LIU Y.-G., LI C.-L., *Plasma loaded free-electron laser with an electromagnetic wave wiggler and axial guide field*, Physics of Plasmas **1**(12), 1994, pp. 4089–93.

[7] DAVIES J.A., DAVIDSON R.C., JOHNSTON G.L., *Compton and Raman free-electron laser stability properties for cold electron beam propagating through a helical magnetic wiggler*, Journal of Plasma Physics **33**, 1985, pp. 387–423.

[8] DAVIES J.A., DAVIDSON R.C., JOHNSTON G.L., *Compton and Raman free-electron laser stability properties for warm electron beam propagating through a helical magnetic wiggler*, Journal of Plasma Physics **37**, 1987, 255–98.

[9] ROBERSON C.W., SPRANGLE P., *A review of free-electron laser*, Physics of Fluids B: Plasma Physics **1**(1), 1989, pp. 3–42.

[10] MISHRA P.K., *Kinetic description of low gain free electron laser using Einstein coefficient method*, Laser Physics **15**(5), 2005, pp. 679–85.

[11] MISRA K.D., MISHRA P.K., *Generalized theory of free-electron laser in a helical wiggler and guide magnetic fields using kinetic approach*, Physics of Plasmas **9**(1), 2002, pp. 330–9.

[12] MISHRA P.K., *A Comparative study of full dispersion relation, Compton dispersion relation and Raman dispersion relation of a free-electron laser in helical wiggler and guide magnetic fields*, Laser Physics **16**(7), 2006, pp. 1050–3.

[13] DAVIDSON R.C., *An Introduction to the Physics of Nonneutral Plasmas*, Addison-Wesley Publishing Company, Massachusetts 1990.

[14] DEMOKAN O., KABAK Y., *Explicit expression for growth rates in free-electron laser with helical and axial magnetic fields*, Physics of Fluids B: Plasma Physics **4**(10), 1992, pp. 3382–9.